1   **Using a Saturation Function to Interpret the Electrical Properties of Partially Saturated Concrete**

2   Jason Weiss,[1] Ken Snyder,[2] Jeff Bullard,[2] and Dale Bentz[2]

3   1 Purdue University, West Lafayette, IN

4   2 National Institute of Standards and Technology, Gaithersburg, MD

5   **Abstract**

6   Electrical properties are frequently measured in the concrete construction industry as a part of
7   mixture qualification and quality control testing. While there are several factors that influence the
8   electrical response of concrete, one of the most important factors is its degree of saturation. Although
9   current standard tests rely on the concrete being saturated, this can be difficult to accomplish, is time
10   consuming, and can artificially increase the degree of hydration of the test sample in comparison to that
11   of concrete in field structures (when the test samples are stored in water). While some studies have
12   measured the electrical response of concrete for samples with different moisture content (i.e., stored at
13   different relative humidities), a single expression has not been proposed that predicts how drying
14   changes the electrical response. This paper suggests that a saturation function should be considered as
15   a possible method to account for, and to correct for, less than complete saturation in concrete. This
16   function would provide one term that accounts for changes in pore fluid volume, pore solution
17   concentration, and pore fluid connectivity. While preliminary, this approach has several potential
18   benefits: 1) it could enable testing of partially saturated concrete, thus saving time; 2) it could be used
19   to predict properties under different exposure conditions; 3) it may facilitate more comprehensive
20   service life models; and 4) it may enable a wider use of embedded sensor technology.

21   **1.   Background**

22   Several test methods exist in the construction industry that use measures of the electrical
23   properties of concrete as an indicator of potential durability performance. The so-called rapid chloride
24   permeability (RCP) test (e.g., AASHTO T277/ASTM C1202) is one example of an electrical test for
25   concrete. For nearly three decades, the concrete profession has qualified concrete mixtures using the
26   RCP testing procedure. While rapid in comparison to long-term ponding tests, the RCP test procedure
27   applies an electrical potential to the test sample for 6 h and requires that the sample be vacuum
28   saturated prior to testing. Several researchers have suggested that the testing time could be
29   dramatically shortened without compromising the quality of the data. Snyder et al. (2000) illustrated
30   that there was no need for the 6 h measurement because values after 1 min or 5 min provide an equally
31   valid indication of the electrical resistivity of the concrete. Other researchers have also confirmed that
32   the test can be performed with shorter test times (Shane et al. 1999, Riding et al. 2008). In fact,
33   shortening the test would improve the quality of the results, as it reduces the potential for Joule
34   heating, which artificially increases the measured response of charge passed over time (Julio-Betancourt
35   and Hooton 2004). Since the time of the preparation of this paper, ASTM committee C09 has accepted a
36   new test method to implement this more rapid measurement protocol (ASTM C1760). But, even if the
37   measurement time is reduced, the sample preparation time is still inconveniently long. RCP testing (or

38 ASTM C1760) requires saturation of the sample, a task which is time consuming, labor intensive, and
39 difficult to accomplish in many cases. The cost of testing (in terms of time and money) could be
40 significantly reduced if reliable measurements could be made on partially saturated specimens. Such a
41 measurement also provides value in that it can provide information on the transport properties under
42 partially saturated conditions.

43   Similarly, time might be saved by using test geometries and methods other than the rapid
44 chloride permeability test. Surface measurements of electrical properties are popular (FM-5-578 2004)
45 and AASHTO has recently developed a provisional standard (TP95-11) based on the Wenner four probe
46 surface resistance test (Morris et al. 1996, Berke and Hicks 1992, Kessler et al. 2005, UNE 2008a, Jackson
47 2011, Rupnow and Icenogle 2011). Although this test procedure can be performed in less than 2 min, it
48 frequently requires the storage of samples in lime saturated water. While storage in water is intended
49 to ensure that the samples are saturated, low-permeability concretes may not maintain saturation even
50 after long immersion times, due to self-desiccation (internal drying). Likewise, samples stored in air,
51 even humid air, are not fully saturated. Furthermore, storage in water may provide additional curing
52 and/or leaching that are not representative of what may be happening in actual field structures.

53   Other test procedures have also been proposed for rapid electrical testing. Specifically, a test
54 procedure has been proposed that measures a bulk resistivity through cylinders (Whittington et al.
55 1981, Newlands et al. 2008, UNE 2008b, Spragg et al. 2011). Tests could be conducted on samples of
56 other geometries or even between embedded electrodes (Monfore 1968, McCarter et al. 1981, Hansson
57 and Hansson 1983, Christensen et al. 1994, Tumidajski et al. 1996 , Gu et al. 1992, Raupach and Scheissl
58 1997, Scheissl et al. 1999, Sellevold et al. 1997, Shane et al. 1999, Weiss et al. 1999, Rajabipour et al.
59 2007, Poursaee et al. 2009, Castro et al. 2010). Each of these methods uses a different electrode
60 configuration and sample size, thereby requiring a separate geometric correction factor; however, the
61 fundamental principles of the tests are similar. Details on many of the geometric correction factors are
62 available in the literature (e.g., Rajabipour 2006).

63   It is interesting to note that, when the appropriate geometric corrections are made and the
64 samples are uniform (i.e., relatively homogenous) and properly conditioned, an intrinsic material
65 property (conductivity or resistivity) is obtained that is independent of sample geometry. Therefore, all
66 of these methods have great promise for moving the field towards qualification and quality control test
67 methods that are simple and related to durability performance, but it should be noted that their results
68 can be dramatically influenced by the degree of saturation of the concrete (Monfore 1968, Scheissl et al.
69 1999, Andrade et al. 2011). This paper will focus on understanding how the moisture content (i.e.,
70 degree of saturation) influences the overall measured electrical response. Specifically, this paper
71 suggests that a universal expression could be used to interpret measurements for partially saturated
72 concrete.

73 **2.   Electrical Conductivity Expression for Saturated Concrete**

74   The electrical conductivity (inverse of resistivity) of concrete depends on four factors: the
75 conductivity of the solution in the pores, the volume of saturated pores (porosity), their connectivity

76 within the microstructure (tortuosity), and the degree of saturation. Although there are several
77 expressions that could be used to estimate the electrical response of a composite like concrete
78 (Torquato 2002), the two most commonly used are a modified parallel law (Garboczi 1990) and Archie's
79 equation (originally developed in 1942 and reprinted in 2003). Of the two, Archie's equation for the
80 electrical conductivity of a rock soaked (saturated) in brine provides a useful starting point:

$$\frac{\sigma_r}{\sigma_b} = a\phi^m$$
[1]

81 where a is a parameter that depends upon the rock type, σ_r is the rock conductivity, σ_b is the brine
82 conductivity, and ϕ is the pore volume fraction (porosity). The exponent m is a fitting parameter that is
83 referred to as the cementation factor. It should be noted that the cementation factor refers to how the
84 microstructure is formed, and is not related to the actual cementitious content of the material.

85 **3.   Electrical Conductivity Expression for Partially Saturated Concrete**

86   Several researchers have developed expressions similar to equation 1 for partially saturated
87 concrete. These modifications consist of reinterpreting the pore volume as only the volume of the pore
88 fluid (Weiss 1999, Andrade et al. 2011).   While that simple correction may be expedient, it leads to
89 some confusion between pore volume and fluid-filled pore volume. Further, additional complications
90 arise since several factors in Eq. 1, including the pore solution conductivity and solution connectivity,
91 change as the degree of saturation changes. As such, previous work has accounted for each factor
92 individually (Rajabipour et al. 2007); however this can be very time consuming and does not lend itself
93 to easy use for quality control testing.

94   An alternative approach is to start with the expression that characterizes the pore structure of
95 the concrete called the formation factor (a uniquely defined parameter for a material with a given
96 composition and degree of hydration) and to incorporate the effects of partial saturation. For a fully
97 saturated concrete, the ratio of the pore solution conductivity at saturation σ_p^o to the concrete
98 conductivity at saturation σ_c^o is the formation factor F (Snyder, 2001):

$$\frac{\sigma_p^o}{\sigma_c^o} = F$$
[2]

99   For a partially saturated concrete, the concrete conductivity σ_c decreases as the saturation level of the
100 concrete decreases. This is due, in part, to the reduction in the pore fluid volume but also due to
101 changes in the connectivity of the connected pathways and changes in the pore solution in the system
102 (Rajabipour et al. 2007). For a concrete, the relationship between the concrete conductivity and the
103 saturation could be accounted for using an expression that will be referred to as the saturation factor,
104 *f(S)*:

$$\frac{\sigma_c}{\sigma_p} = \frac{1}{F} f \ S$$
[3]

105 Furthermore, if one assumes that the pore solution at saturation (σ_p^o) is known, the pore solution
106 conductivity at values other than saturation (e.g., due to drying) can be (at first approximation) related
107 to the degree of saturation as:

$$\sigma_p = \frac{\sigma_p^o}{S} \qquad\qquad [4]$$

108   Combining equations 3 and 5 results in equation 5:

$$\sigma_c = \frac{\sigma_p^o}{S} \; \frac{1}{F} \; f \; S \qquad\qquad [5]$$

109   While the left hand side of the equation is the conductivity of the concrete as a function of saturation,
110   the right side of the equation has three terms. The first term accounts for the pore solution conductivity
111   (due to the mixture design and subsequent concentration due to water loss), the second term accounts
112   for the total pore space and the third term accounts for the connectivity of the fluid in the pore space.
113   Each term is independent of the others, and all of the parameters are related to well defined properties
114   of the matrix and the solution filling its pores.

115   The saturation function is used in other transport problems and could be formulated in a number of
116   ways (Millington and Quirk 1961, Martys 1999, Samson and Marchand 2008,
117   (http://en.wikipedia.org/wiki/Archie%27s_law)). Although there is flexibility in how the saturation
118   function is formulated, the constraint is that at saturation (S=1), the function's value is unity (f(S=1)=1).
119   One viable function that has been used to describe the influence of saturation is a power-law
120   relationship:

$$f \; S \; = S^n \qquad\qquad [6]$$

121   where n is a fitting parameter called the saturation coefficient. As described later in this paper, n is
122   typically of the order of 1.5 to 3 for rocks, while it may be slightly higher for cement and concrete (i.e., in
123   the range of 3.5 to 5 for the paste and mortar samples discussed in this paper and 5 for the computer
124   simulations discussed in this paper).

125   It should also be mentioned that the degree of saturation (S) is frequently determined using the
126   difference in mass before and after drying at 100°C normalized by the equivalent difference in mass for
127   a saturated system. This mass-based form of the degree of saturation is used since it is easy to
128   determine experimentally in the laboratory. But, the mass-based determination is equal to the
129   saturation in terms of fluid volume only if the filling liquid is water. For concentrated electrolytes such
130   as concrete pore solutions, there may be merit in interpreting S as a volumetric degree of saturation
131   (volume of the fluid as compared with the overall volume of fluid that can be held by the pore system of
132   the sample at saturation).

133   Figure 1 shows a plot of the saturation function S^n along with estimates based on experimental
134   data from Rajabipour et al. (2007), calculated from Eq. 3 using known values for the pore solution
135   conductivity at each step. In figure 1, the degree of saturation was determined on a mass basis. As may
136   be expected, the cement system behaves slightly differently than the siltstone that has larger pores, few
137   if any 'ink bottle pores', and a more open pore network. The saturation coefficient for the siltstone is
138   approximately 2 (which is a value consistent with that reported in the geological literature
139   (Schlumberger Oilfield Glossary 2011)). However, for the cement-based system with a ratio of water
140   mass to cement mass (w/c) of 0.50, the value of the saturation coefficient is approximately 3.5, and the
141   saturation coefficient approaches 5 for the system containing silica fume (w/c = 0.35 + 5 % silica fume).

142 The saturation function shown as the dashed line in Figure 1, using equation 6, assumes n = 4. It should
143 be noted that the saturation function shown in Figure 1 is equivalent to the normalized conductivity
144 (ratio of the conductivity of the concrete to the conductivity of the pore solution). As such, data like
145 those in Figure 1 are currently quite rare in the concrete literature, as the changes in the pore solution
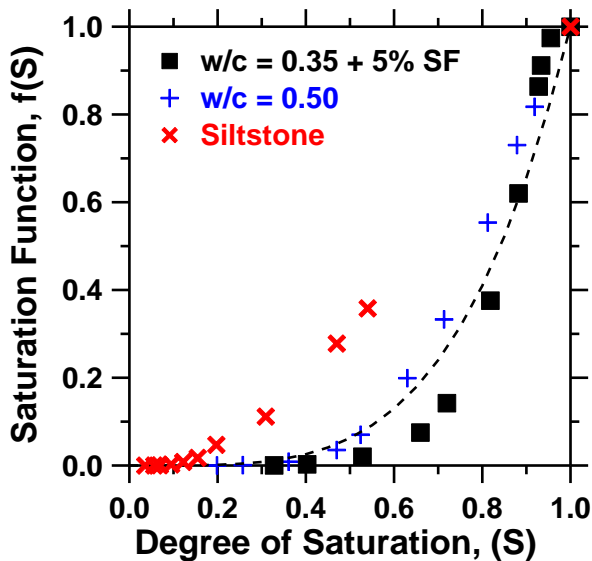146 with saturation must be included when developing such data.

147

148 Figure 1: Experimentally Measured Saturation Coefficients for Siltsone and Cementitious Materials.
149 (Containing data from Rajabipour 2006)

150 **4. Saturation Functions from Simulation (Considering pore fluid volume and connectivity)**

151   The Virtual Cement and Concrete Testing Laboratory software (VCCTL), used to predict degree
152 of hydration, microstructure development, and physical properties of cement paste, mortar, or concrete
153 (Bullard et al., 2008), was adapted in this study to estimate the form of a saturation function. One
154 advantage of the numerical simulations is that they automatically account for the pore solution
155 conductivity, a property which may be difficult to measure experimentally in many partially saturated
156 cementitious samples for three reasons. First, it becomes difficult to extract the pore solution using the
157 pressurized approach like the one proposed by Barneyback and Diamond (1981) in partially saturated
158 conditions, due to the very low volume of available pore fluid. Second, the loss of water by drying can
159 also increase the ionic concentration of the solution, which concurrently increases the pore solution
160 conductivity (Rajabipour et al. 2007). Finally, pore solutions can be susceptible to rapid carbonation,
161 which will also significantly alter their conductivity (Rajabipour 2006).

162   Using the VCCTL, 3D virtual microstructures of cement paste were generated that were
163 chemically and physically representative of the real systems considered in this paper. Hydration and
164 microstructure development, under either saturated or sealed moisture conditions, were simulated out
165 to ages of 1 d, 2 d, 3 d, 7 d, 28 d, 90 d, and 365 d. The 3D microstructures at each age were input into a
166 finite difference model that calculated the net charge flux across the microstructure in response to a
167 fixed applied electric field. The relative conductivity of the microstructure was computed by dividing the

168 charge flux by the electric field (Ohm's law). In addition, the formation factor, F, was calculated by
169 saturating the capillary pore volume (for the sealed curing condition specimens) and repeating the
170 calculation of effective conductivity.

171   Figure 2 shows the simulated cement paste microstructures for a sealed mortar with a *w/c* of
172 0.42 and an aggregate volume fraction of 55 % at 3 d (Figure 2a) and at 365 d (Figure 2b). Over time, the
173 capillary porosity of the system decreases due to hydration. In addition, since the system is sealed, the
174 vapor-filled space increases due to chemical shrinkage and self-desiccation. To estimate the saturation
175 function, the conductivity of the sealed mortar was compared with the sealed mortar that was
176 'resaturated' by altering the conductivity of the vapor-filled space to be equivalent to that of the pore
177 solution.

178

179   (a)   (b)
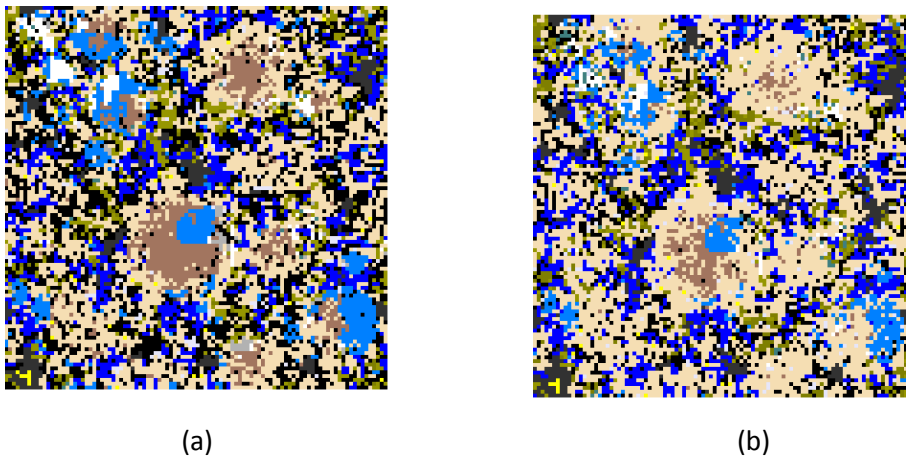
180 Figure 2: Microstructural images developed using the VCCTL model for a mortar with a *w/c* of 0.42 and
181 an aggregate volume of 55 % at a) 3 d and b) 365 d hydrated under saturated conditions. The phases
182 are color-coded as follows: black = capillary porosity, brown = alite, light blue = belite, white = ferrite,
183 beige = C-S-H gel, dark blue = CH, and green = ettringite and monosulfoaluminate combined.

184   It should be noted that two types of porosity are generally considered to exist in a hydrated
185 cement paste system. The capillary pores are larger pores (shown in black in Figure 2) which remain
186 from the original space occupied by mix water that has not filled in during hydration. The gel pores are
187 smaller pores that are created within hydration products.   In the VCCTL model, microstructure is
188 represented as a 3D digital image where each voxel, a 1 μm cube, is assigned a particular cement phase.
189 Therefore, capillary pores are computed directly from the voxels that represent pores in the simulation,
190 but the gel pores are assumed to occupy 38 % of the volume of any C-S-H voxel. This compares
191 favorably and is consistent with the calculations from a Powers' model type approach (Powers and
192 Brownyard 1942). An advantage of the VCCTL model as compared with the Powers' calculations is that
193 it provides a 3D spatial distribution of the porosity, including its tortuosity, which can be used in
194 conductivity computations. A disadvantage is that the capillary pores have a lower size limit of 1 μm
195 because of the finite voxel size. This lower limit is relatively coarse compared with the smaller capillary
196 pores in a typical hydrated portland cement, although comparisons of capillary porosity correlation

197 functions determined on model and real microstructures for a *w/c*=0.47 cement paste are quite
198 favorable (Bentz 2006).

199   Figure 3a shows results from the VCCTL simulation of a paste with a *w/c* of 0.50 and a degree of
200 hydration of 65 % yielding a similar formation factor (24.2) as that from the experimental data shown in
201 Figure 1. A series of simulations were subsequently performed where fluid was systematically removed
202 from the capillary pores to simulate the influence of a change in the degree of saturation caused by
203 drying, by emptying the largest pores within the 3D microstructure first, consistent with the algorithm
204 currently employed for self-desiccation of microstructures hydrated under sealed conditions. While the
205 general trend between the experiment and the simulation is similar, it can be noticed that the
206 simulation shows a more dramatic influence of drying on the saturation function than is observed
207 experimentally (n = 5 for the simulations, while n = 3.5 for the experiment shown in Figure 1).

208   Figure 3b plots the simulated saturation function for a series of sealed specimens with different
209 *w/c*'s. The saturation function was determined by using the conductivity of a sealed mortar and the
210 conductivity of that sealed mortar after being 'resaturated', (i.e., by altering the conductivity of the
211 vapor-filled space to be equivalent to that of the pore solution). The results in Figure 3b represent
212 mortars with a wide range of *w/c* (0.30 to 0.45) and ages of 3 d to 365 d, along with the 0.50 paste that
213 was dried after reaching 65 % hydration (as shown in Figure 3a). The results of these simulations appear
214 to collapse reasonably close to the same line (*n*=5).

215   While these results indicate the potential that a single function may work for cementitious
216 systems (with *n* equals approximately 4 from the limited experimental data), it should be noted that an
217 exhaustive examination of all cement compositions, particle size distributions and degrees of hydration
218 were not considered, as small changes in *n* may be observed. It is recommended that experiments be
219 performed over a wide range of concrete mixture compositions to determine the best choice for this
220 saturation coefficient.

221

222

223   (a)   (b)
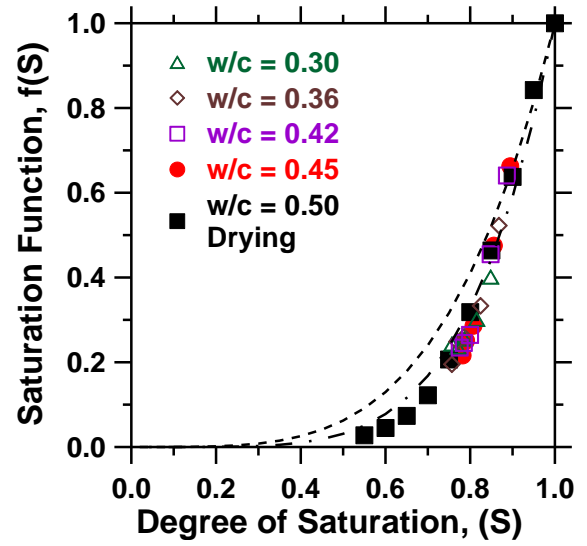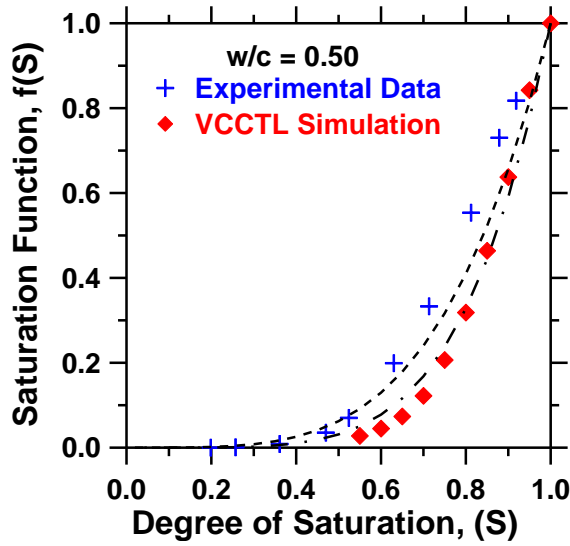
224   Figure 3: a) A Saturation Function Interpreted for VCCTL computer simulations b) Calculated saturation
225   functions obtained from a series of simulated microstructures. The dashed curve corresponds to a
226   saturation coefficient n=4 and the dotted and dashed line corresponds to a saturation coefficient n=5.

227   **5.   Correction for High Pore Solution Concentration on Drying**

228   The parameter S appearing in Eq. 4 approximates the influence of the water loss from the pore solution
229   which increases concentration and conductivity (e.g. due to drying). It is mentioned that equation 4 is a
230   good first approximation for the pore solution conductivity; however, it does not account for the
231   nonlinear relationship between conductivity and concentration that arises from ionic interactions. A
232   more thorough expression can be developed based on the work of Snyder (2001). While the full
233   derivation that is provided in Snyder (2001) was used in the analysis here, a simplified version is
234   presented that produces nearly identical results where the conductivity of the solution is assumed to be
235   proportional to the ionic strength (I_M, based on molar concentration) of the solution with a single
236   correction parameter for high ionic strengths:

237            $$\sigma \propto \frac{I_M}{1 + G\,\overline{\overline{I_M}}}$$ [7]

238   where G is the conductivity parameter (assumed to be approximately 0.4 $(mol/L)^{-1/2}$ for a typical pore
239   solution). Starting at saturation, as the specimen dries, the ionic strength is inversely proportional to
240   the saturation (this is the same as increasing the concentration). The ratio of the pore solution
241   conductivity to the initial pore solution conductivity is given in equation 8. The expression in equation 8
242   can be approximated by a power-law relationship where the degree of saturation is raised to a
243   correction exponent, δ-1 where the value of δ is a function of the pore solution ionic strength as shown
244   in Figure 4.

245
$$\frac{\sigma_p}{\sigma_p^o} \cong \frac{1}{S} \; \frac{1+G \; \overline{I_M}}{1+G \; \frac{1}{S} \; \overline{I_M}} = S^{\delta-1} \qquad\qquad [8]$$
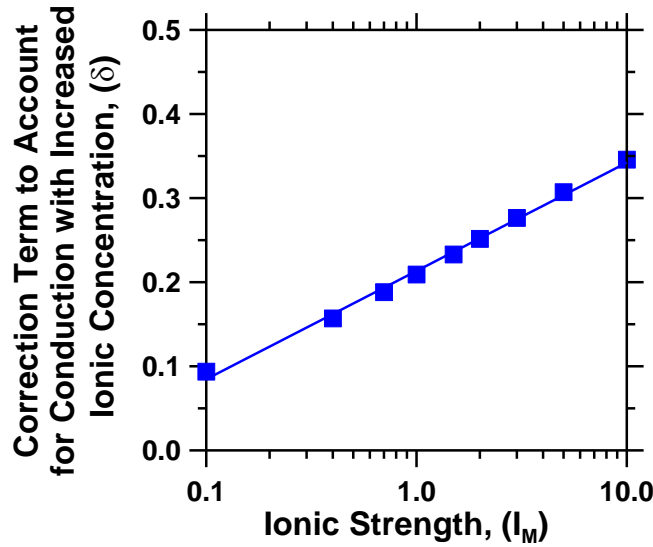
246

247 Figure 4: A Correction term (δ) to account for the ionic interactions in a pore solution, having an ionic
248 strength I_M when the sample is saturated, as it becomes more concentrated due to drying

249 Combining equations 2, 3, and 8 yields a result for the ratio of the conductivity of drying concrete to
250 saturated concrete accounting for the saturation coefficient and the concentration of the pore solution
251 due to drying, where δ is based on the ionic strength:

$$\frac{\sigma_c}{\sigma_c^o} = S^{n-1+\delta} \qquad\qquad [8]$$

252 Therefore, once the value of δ has been determined by either direct measurement of the pore fluid ionic
253 strength or by estimation based on the mixture design (i.e., the ionic strength), and assuming that n is
254 known for a material or there exists a universal value of *n* for concrete, one can use equation 8 to
255 estimate the change in a concrete conductivity due to changes in its degree of saturation.

256 **6.   Example Application 1 - Comparing Sealed and Saturated Curing Conditions**

257   To illustrate the need for a method that enables electrical conductivity measurements to be
258 corrected based upon the degree of saturation in the concrete, the variation in conductivity was
259 measured from a series of concrete cylinders that were cast along with a bridge deck, made with an
260 ordinary portland cement concrete having a *w/c* of 0.39. These cylinders were demolded at 24 h and
261 were stored for a year (DiBella et al. 2011). The concrete cylinders were conditioned in one of three
262 ways after demolding. First, some samples were stored in lime water after demolding to simulate water
263 curing. Second, other samples were sealed in a double layer of thermally sealed plastic bags. The
264 samples that were sealed in bags were removed from the bags and tested in the sealed state. The
265 degree of saturation for the concrete sealed in a bag after 1 year was measured to be 0.56, which
266 corresponds to a relative humidity of approximately 85 % to 90 % (Li et al. 2012). Third, after initial

267   testing, the sealed concrete samples were then cut to size for RCP testing and water saturated under
268   vacuum in accordance with the ASTM C1202 procedures. Before conducting the 6-h measurement in
269   ASTM C1202, the resistivity was measured using plates on either side of the concrete disk (52 mm tall by
270   102 mm in diameter). At an age of 365 d, the measured conductivity of the concrete stored in lime
271   water was 0.0143 S/m.   In contrast, the sealed concrete conductivity was 0.0037 S/m, and after being
272   resaturated, its conductivity was 0.0296 S/m, which is eight times greater than before resaturation.
273   These values are shown in Figure 5. Therefore, the measured conductivity strongly depends on how the
274   sample was cured and conditioned prior to testing.

275   This sensitive dependence of conductivity on sample storage and preparation implies that there
276   are at least two potential pitfalls when interpreting these kinds of measurements, both of which can
277   cause an underestimation of the conductivity. First, if a conductivity measurement were made on a
278   partially saturated sample, one could naively (and mistakenly) believe that the material has a
279   conductivity (diffusivity) that is nearly an order of magnitude better (i.e., lower) than it actually is (when
280   saturated). The second pitfall is to neglect the effect of storage conditions. The concrete stored in lime
281   water has approximately half the conductivity of the concrete that was sealed during curing and
282   saturated at the time of testing. Therefore, a sample stored in lime water in the laboratory would
283   appear to be performing much better than the same concrete in the field if the curing/sealing
284   compounds were working perfectly (and the concrete was saturated when sealed and when tested).

285   A mortar similar to that used in the experiments shown in Figure 5 was modeled using the
286   VCCTL (w/c of 0.39 and an aggregate volume of 55 %). The simulation should not be compared directly
287   to the field concrete since it was performed on mortar and did not include entrained air. The simulation
288   is still helpful, however, since it can provide some useful insights regarding trends and for interpreting
289   the results as a function of their curing conditions and the saturation function.   The simulated
290   normalized conductivity obtained using the VCCTL is 0.00047 for the lime water saturated specimen,
291   0.000266 for the sealed specimen, and 0.00134 for the sealed sample that was resaturated.   The
292   conductivity of the pore solution was estimated using an equivalent sodium content of 0.67
293   (http://concrete.nist.gov/poresolncalc.html; Bentz (2007)) with a resulting pore solution conductivity
294   between 12.4 S/m and 14.9 S/m. These estimated mortar conductivities are also shown in Figure 5.
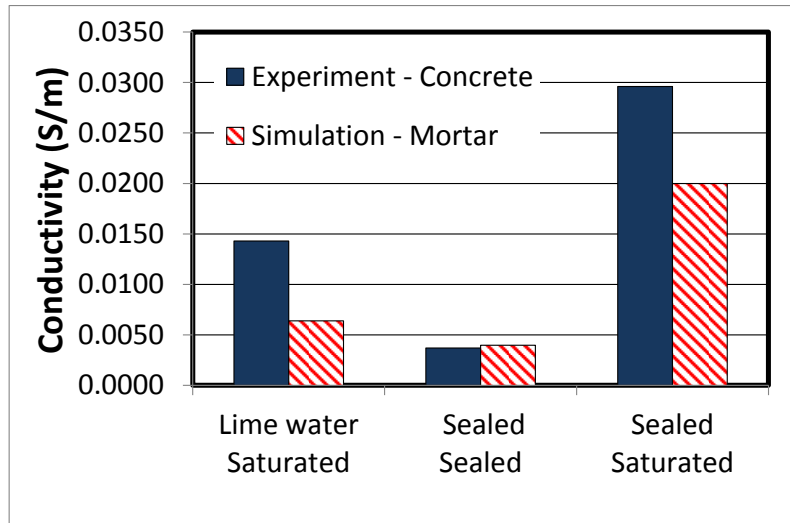
295

Figure 5: Measured electrical conductivity from RCP tests using a field concrete and simulated mortar
with a w/c of 0.39 under different curing and sample conditioning (A maximum coefficient of variation
of 3.2% was observed for the experiments)

In comparing the sample that was continuously stored in lime water with the sample that was
sealed and saturated at each age, the overall conductivity of the continually saturated sample is lower,
presumably due to the differences in the extent of hydration. Figure 6a shows the simulated degree of
hydration as a function of time as obtained from the VCCTL simulations. As one may expect, the system
that is saturated has a higher degree of hydration (87 % at one year) than a system that is simply sealed
cured (75 % at one year) (Bentz and Stutzman 2006). In this particular experiment, the lime-water cured
sample will have a lower porosity (albeit a relatively small decrease from 38 % of the paste to 36 % of
the paste volume fraction). It should be noted, however, that this small reduction in porosity is actually
a relatively large reduction in the fraction of the capillary porosity. For the mixtures being discussed,
nearly 65 % of this porosity at this degree of hydration is gel porosity. Figure 6b illustrates the degree of
saturation in the simulated mortars. While the saturated sample from the simulation remains at 100 %
saturation, the sealed sample has a degree of saturation that progressively decreases to approximately
0.81 at an age of 1 year. It should be noted that the VCCTL simulation did not include entrained air
which would comprise approximately 20 % of the **paste** volume for this mixture. If the degree of
saturation for the concrete sample is adjusted to account for entrained air, the degree of saturation of
the concrete cylinder is more similar to that of the simulation (approx. 0.76 vs. 0.81).

The normalized conductivity for the simulated mortar is plotted as a function of time in Figure
7a. This is similar to results previously shown by Bentz (1998). It can be noticed that the samples have a
similar conductivity at early ages as one may expect; however over time substantial differences in
conductivity begin to develop. To better illustrate the influence of the degree of hydration on the
resulting pore structure, the normalized conductivity is plotted in terms of total pore volume in Figure
7b. Figure 7b shows that a single curve begins to appear that describes the specimens with water
(saturated) curing and the samples with sealed curing when they are tested in a saturated state. This
again confirms that the 'formation factor' (a normalized conductivity/pore solution conductivity) is a

323 material property that varies with degree of hydration (or pore volume) for the saturated system. The
324 primary difference between the samples cured under lime water and the samples that were sealed and
325 resaturated is that the samples that are cured under lime water exhibit more hydration, thereby
326 achieving a lower porosity and a lower normalized conductivity than the sealed/resaturated sample at
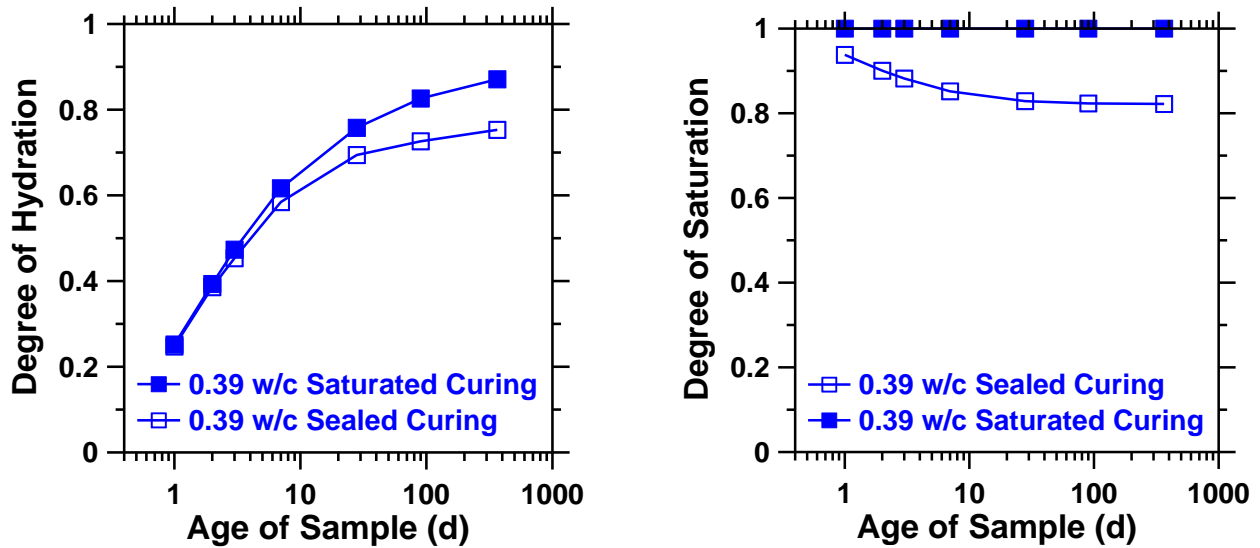327 the same age (Figure 7b). Again, this is consistent with the experimental observations.

328

329   (a)   (b)
330 Figure 6: Mortar with a w/c of 0.39: a) Degree of hydration and b) Degree of saturation

331

332   (a)   (b)
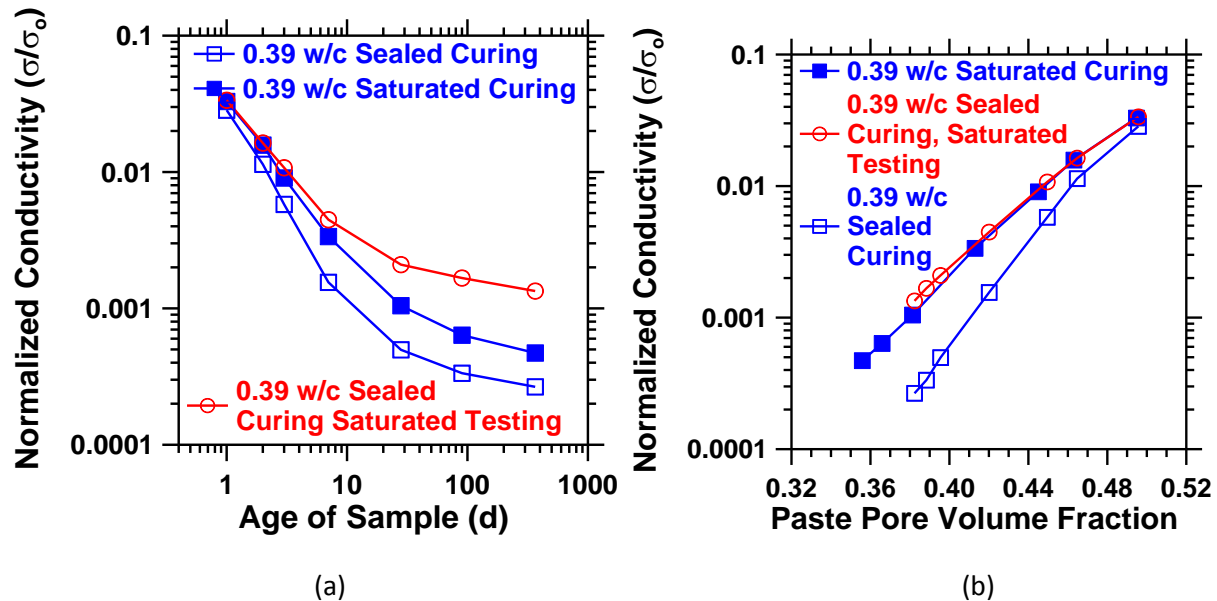333 Figure 7: Normalized conductivity of mortar with a w/c of 0.39: a) as a function of time and b) as a
334 function of the pore volume in the paste as computed using Powers' model

335   The results from Application 1 show that while the electrical conductivity may be a simple
336 property to measure, it can be significantly influenced by curing conditions (sealed versus lime water

337 saturated) and sample preparation (testing the sealed sample versus testing the sealed sample that was
338 resaturated).

339 **7.0   Example Application 2 - Measurements Made on Samples Exposed to Drying**

340   In addition to using electrical property measurements on quality control samples, several
341 researchers have measured electrical properties in concrete systems exposed to drying or wetting
342 (Schieβl 1999, Weiss et al 1999, 1999b, Sellevold 2000, Andrade et al. 2011). While the drying process
343 takes place over a long time period and may set up moisture gradients inside of the concrete (Weiss et
344 al. 1999 and Rajabipour et al. 2005), moisture gradients are not considered here. The saturation
345 approach may be useful in estimating the response of a concrete equilibrated to different levels of
346 drying.

347   Figure 8 illustrates equation 8 plotted as a function of relative humidity (RH) for a series of
348 concretes with a *w/c* of 0.4 that were allowed to dry for nearly a year (Weiss et al. 1999). The equation
349 with a saturation coefficient of n = 4 provides a reasonable shape response at higher humidities, but this
350 relationship begins to break down for RH less than approximately 60 %. At these lower relative
351 humidities, the saturation function is low (approximately 0.1) and the capillary pore water is likely lost,
352 suggesting that the main conduction pathway likely changes from the large capillary pore network to the
353 gel pores or along the walls of the capillary pores. If this is true, the breakdown of the relation valid at
354 higher RH is not surprising.

355   The data for samples with a *w/c* of 0.4 and having no chemical admixtures (Schiessl et al. 1999)
356 were compared with equation 8 and a saturation coefficient of 3.9 was obtained for concrete with a *w/c*
357 of 0.4 for data at relative humidities greater than 60 %. A similar assessment of the data reported by
358 Andrade et al. (2011) would be consistent with saturation coefficients that are approximately 3.5. These
359 coefficients are similar to those observed from the numerical simulations reported in Figures 3 and 4
360 and from the plain pastes in Figure 1. This suggests that this approach may be applicable to drying
361 samples. Figure 8b illustrates the desorption isotherm to relate relative humidity and the degree of
362 saturation. It also illustrates the saturation function (assuming two different values for the saturation
363 coefficient (i.e., n = 4 and n = 5)). This illustrates that once the relative humidity drops below 65 % to 70
364 % RH, the saturation function is very low.

365   As such, it appears that it may be quite reasonable to design an experiment where the
366 saturation coefficient is determined for a concrete mixture by measuring the conductivity of a sample
367 with two different degrees of saturation (provided they are relatively high).   For example, this could
368 consist of measuring the conductivity of a sealed sample and then measuring the conductivity of the
369 same sample after vacuum saturation. Assuming the mass of the sample is measured along with the
370 electrical properties, the degree of saturation could be obtained by oven drying the sample after testing
371 and measuring its oven-dried mass. This could then provide an estimate of *n* for each mixture.
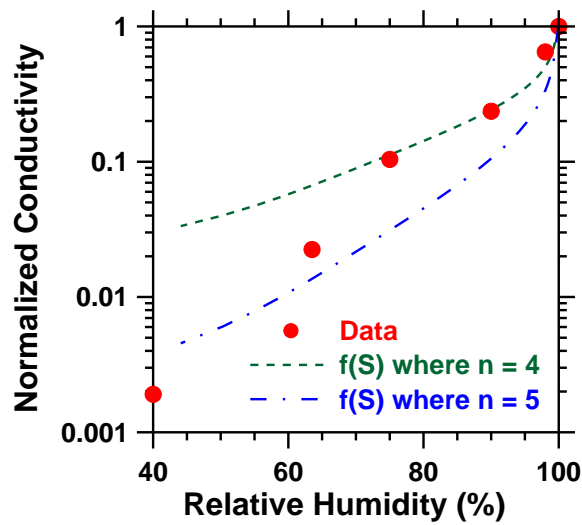
(a)
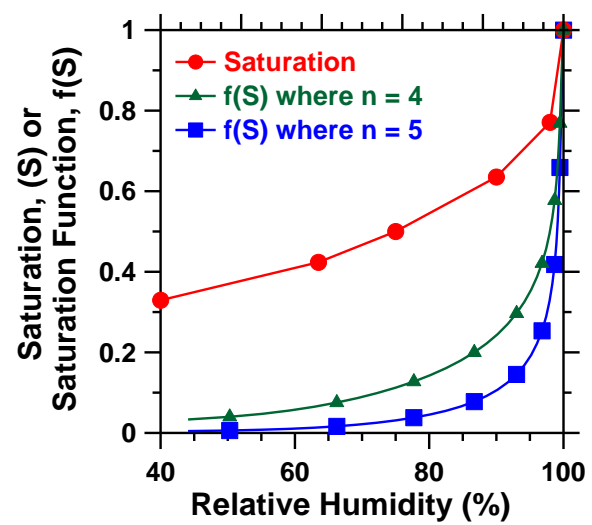
(b)

Figure 8: a) Normalized Conductivity as a Function of Drying and b) The Relationship Between Relative Humidity and Saturation for the Data

A further illustration of this approach can be seen in Figure 9 where the surface resistivity was measured on mortar specimens exposed to drying at 50 +/- 2% relative humidity (1 in. (25 mm) square cross section and a 10.6 inch length (262.5 mm) (Bentz et al. 2012)). It can be noticed that despite the samples not being in equilibrium during the test (i.e., the samples were drying and likely continuing to hydrate slightly) a similar trend emerges for the saturation function. The mixture with a lower w/c would be expected to have a more uniform moisture content and follow the expected function a little more closely than the samples with a higher w/c that likely show some influence of the moisture gradients.
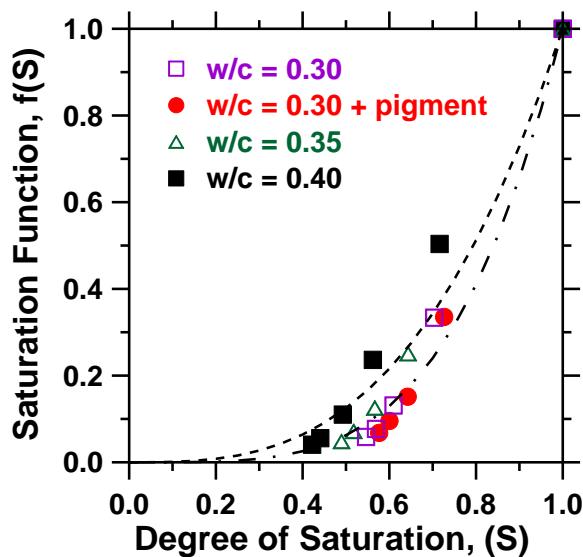

Figure 9: The application of the saturation function to mortar prisms during drying (The dashed line and dot-dash line denotes a n-1+δ value of 3 and 4, respectively).

387

8.0   Summary

388   **8.0   Summary**

389   Tests that measure the electrical conductivity of concrete are sensitive to the degree of
390   saturation of the concrete. This paper explores the potential for testing partially saturated concrete and
391   correcting this data based on its measured degree of saturation to obtain the formation factor, which is
392   a material property. This could have substantial impact when rapid field tests or embedded sensors are
393   used to provide measures of properties related to durability performance. Similarly, this approach could
394   be used to solve the equally important problem of converting measured transport coefficients for
395   saturated concrete to values that would correspond to field conditions with a lower degree of
396   saturation.

397   This paper suggests that the general form of Archie's Law can be written in a way that describes
398   the electrical conductivity of partially saturated concrete, using a stand-alone saturation function. It
399   appears that the saturation function can be written as the degree of saturation raised to an exponent
400   called the saturation coefficient (n). A suggestion for the form of this equation is shown in equation 8
401   which accounts for both drying effects and changes in the pore solution concentration and conductivity
402   during drying. While the saturation coefficient varies from approximately 1.5 to 2.5 for many rocks
403   (shown in this paper for siltstone as 2), it is slightly higher for cement-based materials, ranging from
404   approximately 3.5 to 5.5 for the limited data from experiments. Simulations made using the VCCTL
405   show a coefficient of approximately 5; however these simulations also showed that the saturation
406   coefficient exhibited little variation with changes in the degree of hydration or the water to cement
407   ratio, over the ranges investigated. The use of a saturation value of 4 provided reasonable correlation
408   with the limited experimental data for the plain portland cement-based systems described in this paper.

409   The saturation function in equation 8 accounts for changes in pore solution, pore fluid volume
410   and pore connectivity. The saturation function was used in two examples where the electrical
411   properties were measured, the first being concrete exposed to sealed curing and the second being
412   concretes and mortars exposed to drying. Future studies should be conducted to better understand the
413   response of partially saturated concrete and to obtain experimental values for n for a wider range of
414   concrete mixture compositions. When this work is performed, it would be helpful to describe the pore
415   solution conductivity (or to report the sodium and potassium alkali contents of the cement), so that the
416   role of pore solution concentration can be estimated. It would also be helpful to provide the degree of
417   saturation of the concretes in addition to their measured internal relative humidity.

10.0   References

Andrade, M. C., Bolzoni, F. and Fullea, J. (2011). "Analysis of the relation between water and resistivity isotherms in concrete", Materials and Corrosion, Vol. 62(2), 130-138.

Archie, G. E. (2003). "The electrical resistivity log as an aid in determining some reservoir characteristics", SPE Reprint Series, (9-16.

ASTM C1202 (2010). Standard test method for electrical indication of concrete's ability to resist chloride ion penetration, ASTM International, West Conshohocken, PA.

AASTHTO T277 (2007)., Standard method of test for electrical indication of concrete's ability to resist chloride ion penetration, American Association of State Highway and Transportation Officials, Washington, D.C.

Barneyback, S. and Diamond, S.(1981). "Expression and analysis of pore fluids from hardened cement pastes and mortars ", Cem Concr Res 11, 279.

Bentz, D.P. and Stutzman, P.E., "Curing, Hydration, and Microstructure of Cement Paste," *ACI Materials Journal*, **103**(5), 348-356, 2006

Bentz, D. P. (2007). "A virtual rapid chloride permeability test", Cem Concr Compos, 29, 723-731.

Bentz, D.P., "Quantitative Comparison of Real and CEMHYD3D Model Microstructures Using Correlation Functions," Cement and Concrete Research, 36 (2), 259-263, 2006.

Bentz, D. P., Stutzman, P., Sakulich, A., and Weiss, W. J., (2012), "Study of Early-Age Bridge Deck Cracking in Nevada and Wyoming", NISTIR 7841, January 2012.

Berke, N. S. and Hicks, M. C. (1992). "Estimating the Life Cycle of Reinforced Concrete Decks and Marine Piles Using Laboratory Diffusion and Corrosion Data", in,.

Bullard, J. W. , Ferraris, C. F., Garboczi, E. J., Martys, N., Stutzman, P. E. and Terrill, J. E. (2008). "Virtual Cement and Concrete." Chapter 10 in Innovations in Portland Cement Manufacturing. Edited by J.I. Bhatty, F.M. Miller, and S.H. Kosmatka. Portland Cement Association, Skokie, IL.

Bentz, D.P. (1998) "Modelling Cement Microstructure: Pixels, Particles, and Property Prediction," Materials and Structures, 32, 187-195Christensen, B. J., Coverdale, R. T., Olson, R. A., Ford, S. J., Garboczi, E. J., Jennings, H. M. and Mason, T. O. (1994). "Impedance spectroscopy of hydrating cement-based materials: measurement, interpretation, and application", J Am Ceram Soc, 77 , 2789-2804.

Castro, J., Spragg,, R., Kompare, P. and Weiss, W. J. (2010). "Portland Cement Concrete Pavement Permeability Performance", Joint Transportation Research Program, Indiana Department of Transportation and Purdue University, West Lafayette, Indiana.

456 Dibella thesis

457 FM 5-578 (2004). "Florida method of test for concrete resistivity as an electrical indicator of its
458   permeability", Flordia Department of Transportation, Tallahassee, FL.

459 Garboczi,, E. J. (1990). "Permeability, diffusivity, and microstructural parameters: A critical review", Cem
460   Concr Res, 20 , 591-601.

461 Garboczi, E. J. (1998) Finite Element and Finite Difference Programs for Computing the Linear Electric
462   and Elastic Properties of Digital Images of Random Materials. NISTIR 6269; 211 p. December 1998.

463 Gu, P., Xie, P., Beaudoin, J. J. and Brousseau, R. (1992). « A.C. Impedance Spectroscopy 1 : A New
464   Equivalent Circuit Model for Hydrated Portland Cement Paste », Cement and Concrete Research 22,
465   833-840.

466 Julio-Betancourt, G. A. and Hooton, R. D. (2004). "Study of the Joule effect on rapid chloride
467   permeability values and evaluation of related electrical properties of concretes", Cem Concr Res, 34,
468   1007-1015.

469 Hansson, I.L.H. and Hansson, C. M. (1983). « Electrical resistivity measurements of Portland cement
470   based materials », Cement and Concrete Research, Vol. 13(5), 675-683.

471 Jackson,, N. M. (2011). "Results of round-robin testing for the development of precision statements for
472   the surface resistivity of water saturated concrete", Ponte Vedra Beach, Florida.

473 Kessler, R. J., Powers, R. G. and Paredes, M. A. (2005). " Resistivity Measurements of Water Saturated
474   Concrete as an Indicator of Permeability", in: Corrosion 2005, NACE International, Houston, TX.

475 Li, W., Pour-Ghaz, M., Castro, J., and Weiss, W. J., (2012) "Water Absorption and the Critical Degree of
476   Saturation as it relates to Freeze-Thaw Damage in Concrete Pavement Joints," ASCE Journal of Civil
477   Engineering Materials

478 Martys, N.S., "Diffusion in Partially-Saturated Porous Materials," Materials and Structures, 32, pp 555-
479   562 (1999).

480 Millington, R. J., and Quirk, J. P., (1961) 'Permeability of Porous Solids,' Transactions of the Faraday
481   Society, 57, pp. 1200-1207

482 McCarter, W. J., Forde, M. C. and Whittington, H. W. (1981). "Resistivity characteristics of concrete",
483   Proceedings of the Institution of Civil Engineers (London) Part 1 - Design & Construction, 71,
484   107-117.

485 Monfore, G. E. (1968). "The electrical resistivity of concrete", Portland Cement Association, Research
486   and Development Laboratories, Skokie, IL,.

487 Morris, W., Moreno, E. I. and Sagues, A. A. (1996). "Practical evaluation of resistivity of concrete in test
488   cylinders using a Wenner array probe", Cem Concr Res, 26, 1779-1787.

489 Newlands, M. D., Jones, M. R., Kandasami, S. and Harrison, T. A. (2008). ," Sensitivity of electrode
490   contact solutions and contact pressure in assessing electrical resistivity of concrete", Mater Struct,
491   41, 621-621-632.

492 Powers, T. C., and Brownyard, T.L., (1942) 'Studies of the Physical Properties of Hardened Portland
493   Cement Paste', Bulletin 22 Research and Development Laboratories of the Portland Cement
494   Association, Chicago, Illinois (1948)

495 Poursaee, A. and Weiss, W. J.(2009). « An automated electrical monitoring system (AEMS) to assess
496   property development in concrete », Automation in Construction, Vol. 19(4), 485-490.

497 Rajabipour, F., Weiss,, J. and Shane, J. D., Mason, T. O. and Shah, S. P. (2005) Procedure to interpret
498   electrical

499 Rajabipour, F. and Weiss, J. (2007). « Electrical conductivity of drying cement paste », Materials and
500   Structures, Vol. 40(10), 1143-1160.

501 Rajabipour, F. (2006). "Insitu electrical sensing and material health monitoring in concrete structures",
502   Ph.D. Dissertation, Purdue University, West Lafayette, Indiana.

503 Raupach, M. and Schiessl, P. (1997). « Monitoring system for the penetration of chlorides, carbonation
504   and the corrosion risk for the reinforcement », Construction and Building Materials, Vol. 11(4), 207-
505   214.

506 Riding, K. A., Poole, J. L., Schindler, A. K., Juenger, M.C.G. and Folliard, K. J. (2008). " Simplified concrete
507   resistivity and rapid chloride permeability test method", ACI Mater J, 105, 390-394.

508 Rupnow,. T. D., and Icenogle, P. (2011).   "Evaluation of surface resistivity measurements as an
509   alternative to the rapid chloride permeability test for quality assurance and acceptance", Louisiana
510   Department of Transportation, Baton Rouge, LA, pp. 68.

511 Samson, E., and Marchand, J., (2007) 'Modeling the Transport of Ions in Unsaturated Cement-Based
512   Materials,' Computers and Structures, 85, pp. 1740-1756

513 Schissl, A., Weiss, W. J., Shane, J. D., Berke, N. S., Mason, T.O., and Shah, S. P., (2000) "Assessing the
514   Moisture Profile of Drying Concrete Using Impedance Spectroscopy," Concrete Science and
515   Engineering, Vol. 2, pp. 106-116

516 Sellevold, E. J., Larsen, C. K. and Blankvoll, A. A. (1997). « Moisture State of Concrete in a Coastal
517   Ridge », Special Publication, SP170-42, Vol. 170, 823-834.

518   Schlumberger (2011), Oilfield Glossary

519   Shane, J. D., Aldea, C. D., Bouxsein,, N. F. Mason, T. O., Jennings, H. M. and Shah, S. P. (1999).
520   "Microstrucutral and pore solution changes induced by the rapid chloride permeability test
521   measured by impedance spectroscopy", Concr Sc Eng, 1 , 110-119.

522   Shane, J. D. (2000). "Electrical conductivity and transport properties of cement-based materials
523   measured by impedance spectroscopy", Ph.D. Dissertation, Northwestern University, Evanston, IL.

524   Snyder, K.A., (2001) "The relationship between the formation factor and the diffusion coefficient of
525   porous materials saturated with concentrated electrolytes: Theoretical and experimental
526   considerations," Concrete Science and Engineering, 3 (12), 216-224, (2001).

527   Snyder, K. A., Ferraris, C., Martys, N. S. and Garboczi, E. J. (2000). "Using impedance spectroscopy to
528   assess the viability of the rapid chloride test for determining concrete conductivity", J NIST, 105,
529   497-509.

530   Spragg, R, Castro, J., Nantung, T., Parades, M, and Weiss, W. J., (2011) "Variability Analysis of the Bulk
531   Resistivity Measured Using Concrete Cylinders," JTRP Report SPR-3509, FHWA/IN/JTRP-2011/21
532   DOI: 10.5703/1288284314646

533   Torquato, S. (2002). "Random heterogeneous materials: microstructure and macroscopic properties",
534   Springer, New York, NY.

535   TP95-11 (2011) Draft standard method of test for surface resistivity indication of concrete's ability to
536   resist chloride ion penetration, American Association of State Highway and Transportation Officials,
537   Washington, D.C.

538   Tumidajski, P. J., Schumacher, A. S., Perron, S., Gu. P. and Beaudoin, J. J. (1996). « On the relationship
539   between porosity and electrical resistivity in cementitious systems », Cement and Concrete
540   Research, Vol. 26(4), 539-544.

541   UNE (2008a)
542
543   UNE (2008b)
544
545   Weiss, W. J., Shane, J. D., Mieses, A., Mason, T. O. and Shah, S. P. (1999). "Aspects of monitoring
546   moisture changes using electrical impedance spectroscopy", Second symposium on the importance
547   of self desiccation in concrete technology, Lund, Sweden.
548   Whittington, H. W., McCarter, J., and Forde, M. C. (1981). "The conduction of electricity through
549   concrete", Mag Concr Res, 33 , 48-60.